

Electronic Supporting Information

Plasmonic Giant Quantum Dots: Hybrid Semiconductor-Metal Nanostructures for Truly Simultaneous Optical Imaging, Photothermal Effect and Thermometry

Niladri S. Karan, Aaron M. Keller, Siddharth Sampat, Oleksiy Roslyak, Ayesha Arefin, Christina J. Hanson, Joanna L. Casson, Anil Desireddy, Yagnaseni Ghosh, Andrei Piryatinski, Rashi Iyer, Han Htoon, Anton V. Malko, Jennifer A. Hollingsworth

Contents:

Supporting Notes	page 2
Supporting Figure S1	page 5
Supporting Figure S2	page 5
Supporting Figure S3	page 6
Supporting Figure S4	page 7
Supporting Figure S5	page 8
Supporting Figure S6	page 9
Supporting Figure S7	page 9
Supporting Figure S8	page 10
Supporting Figure S9	page 10
Supporting Figure S10	page 11
Supporting Figure S11	page 11
Supporting Figure S12	page 12
Supporting References	page 13

Supporting Notes

Impact of pH on Au-shell formation

For ultra-thin Au shell synthesis, the nanocrystal substrates (in our case: gQD/SiO₂) are incubated with an aqueous solution of HAuCl₄ and NaOH. A mild reducing agent, NH₂OH, is then added to initiate controlled reduction of Au³⁺ to Au⁰ metal. Importantly, the dilute gold incubation solution (0.25 mM) is maintained at pH 6-7, though it is prepared from a more concentrated HAuCl₄ solution (25 mM) that is initially brought to a pH of 9-10 by addition of NaOH (Methods). The chemistry that underlies this selection of a basic pH for the starting HAuCl₄ solution and the subsequent lower pH for the diluted incubation solution is based on consideration of the hydrolysis products of HAuCl₄:



as well as the acid/base chemistry of the PLH amine groups. With respect to the HAuCl₄ hydrolysis chemistry, the five possible Au(OH)_nCl⁻_{4-n} complexes are soluble in water, while Au(OH)₃ may also form as an insoluble precipitate. At pH 9-10, Au(OH)₄⁻ is the dominant species.¹ Significantly, compared to the chlorinated gold complexes, Au(OH)₄⁻ has the lowest tendency to be reduced,² which ultimately favors a more controlled reduction process. Once formed, this species is maintained even as the pH is lowered in the diluted incubation solution. We suggest that the higher nucleophilicity of the OH⁻ ions compared to the Cl⁻ ions ensures that the hydrolysis reaction equilibrium strongly favors reaction products of higher n.

But, why return to a lower pH at all in the diluted incubation solution? A mildly acidic pH is required to ensure that the amine groups of the PLH binding layer (both of the imidazole side chain and the α-amino group) are fully protonated and positively charged (imidazole side chain pK_a = 6.6 and α-amino pK_a = 9.3). In such a state, they are able to electrostatically bind Au(OH)₄⁻ or other anionic products of the AuCl₄ hydrolysis reactions to establish high concentrations of gold precursor at the nanocrystal surfaces. Subsequent addition of the mild reducing agent then affords controlled, heterogeneous nucleation and growth of uniform and thin gold shells, while avoiding separate, homogeneous nucleation of gold metal. If, instead, the incubation solution is maintained at a basic pH, we observe that controlled shell growth is distinctly not achieved. For example, maintaining the diluted incubation solution at pH 9-10

results in the formation of thick Au deposits on some gQD/silica nanocrystals and none at all on others (Supporting Figure 1). At these pH values the nitrogen atoms of the PLH imidazole side chains and α -amino groups are not protonated and could themselves initiate the $\text{Au}^{3+} \rightarrow \text{Au}^0$ reduction process through lone-pair electron donation.^{3, 4, 5} In this case, the Au that is formed is not only thick but it is also not necessarily conformal to the nanocrystal substrates, often forming deposits substantially larger than the starting gQD/SiO₂ nanocrystals, appearing to encompass several (Supporting Figure 1). Where the resulting Au-coated product retains the approximate size and shape of the starting gQD/SiO₂ nanocrystal, it is rough and bumpy (Supporting Figure 1c). Both observations suggest that the gold precursor/substrate interaction is less intimate and less ideal than that enabled under mild acidic conditions. Furthermore, we observe that when the Au reduction step is conducted at even higher pH (>10) $\text{Au}(\text{OH})_4^-$ appears to penetrate the mesoporous silica spacer layer so that Au^{3+} gets reduced at the CdS gQD surface, resulting in Au deposits between the QD and the silica layer.⁶ At these very basic pHs, it also appears that the silica layer is partially etched, but only at the QD interface (Supporting Figure 2). Such localized etching likely results from the formation of high concentrations of OH^- ions upon reduction of $\text{Au}(\text{OH})_4^-$ to Au^0 between the gQD and the silica.

Nevertheless, the initial diversion of the concentrated HAuCl_4 solution to a basic pH of 9-10 is a necessary step. If, instead, the entire process is conducted at $\text{pH} < 7$, a very fast and uncontrolled reduction is observed with nucleation of free Au nanoparticles. Thus, when starting with HAuCl_4 as a precursor for ultra-thin-shell growth, the gold reduction process must be considered as a two-step process: (1) Hydrolysis of the gold chloride species to a less easily reduced form of Au^{3+} and (2) Protonation of nanocrystal-surface amine groups for promotion of ideal electrostatic interactions with a negatively charged gold complex and minimization of amine-initiated gold reduction. The significance of the former step has long been appreciated in literature describing the preparation of oxide-supported Au catalysts¹ and more recently in some thick-shell Au nanoshell work², but the chemistry underlying the use of an initially high pH has not been recognized in the ultrathin-Au shell literature,⁷⁻⁹ despite the clear sensitivity of the resulting solid Au product to the pH conditions employed through the course of the reaction. We emphasize this point here to aid in future efforts directed at cluster-free synthesis of ultrathin-Au shells.

Imaging the ultra-thin Au shell and electron microscopy artifacts

It is possible to generate the “appearance” of a dark, thin ring or apparent shell around the outside of a *pl*-gQD particle by defocusing the low-resolution TEM image (Supporting Figure 3a,b). However, this should not be interpreted as the metal shell itself, as an equivalent effect can be created by applying the same defocusing to a gQD/SiO₂ particle (Supporting Figure 3c,d). In both cases, the dual appearance at sufficiently high defocusing of a higher contrast outer layer and an ~zero-contrast thin intermediate layer (between the dark ring and the particle interior) (Figure 3b) results from the Fresnel effect. We further investigated whether the ‘ring effect’ might develop for lesser degrees of defocusing for Au-shell particles compared to silica-only particles, and thereby afford some direct confirmation and visualization of the metal shell. Instead, we found no such difference between the two types of particles, i.e., for equivalent magnifications approximately the same level of defocusing caused a dark ring to appear.

Supporting Figures

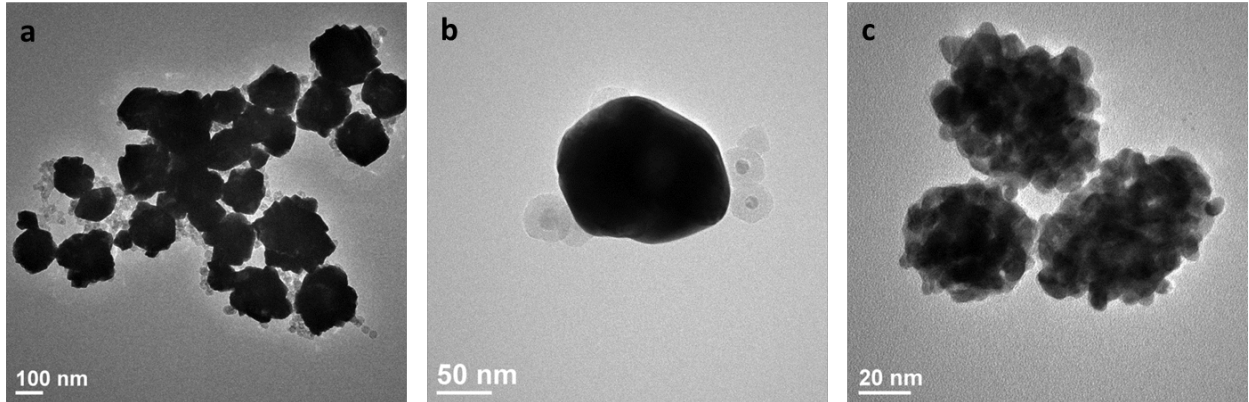


Figure S1. TEM images of the samples obtained from the reduction of Au^{3+} ions at $\text{pH}=9-10$. At this condition thick Au deposits covering many gQD/ SiO_2 particles. Some particles are thickly coated and others are not coated at all. However, the Au shell is not uniform, but, rather, bumpy and rough.

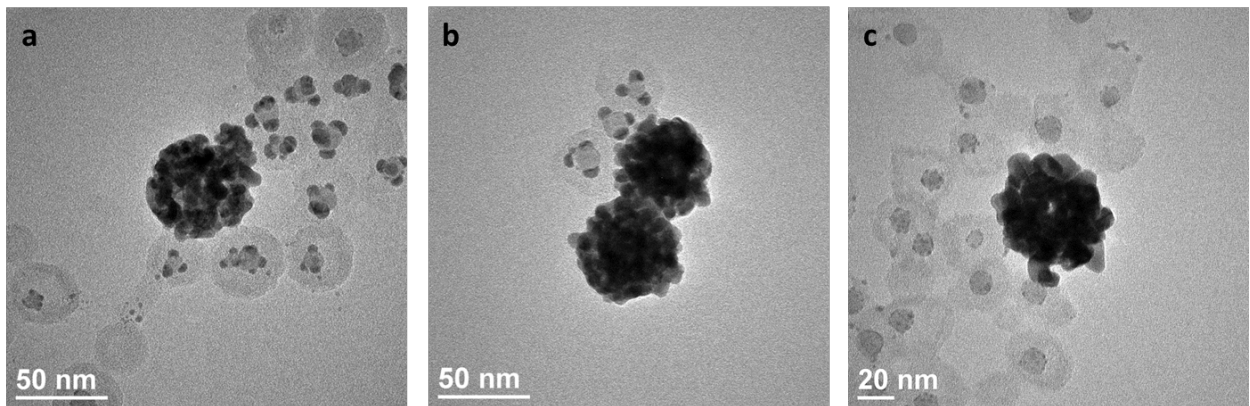


Figure S2. TEM images of the samples obtained from the reduction of Au^{3+} ions at $\text{pH} \geq 10$. $\text{Au}(\text{OH})_4^-$ penetrates through the mesoporous silica leading to inside out etching.

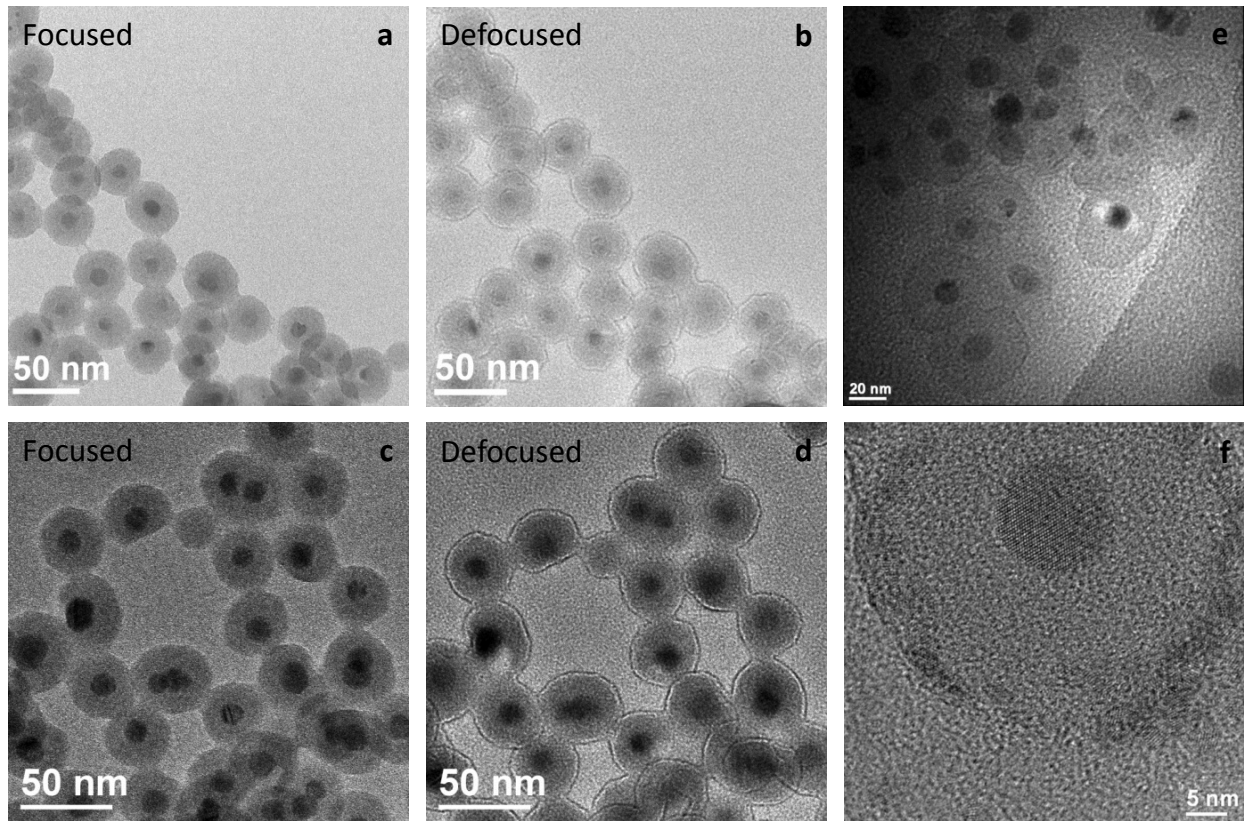


Figure S3. TEM image of the *pl*-gQD samples under focused (a,c) and (b,d) defocused condition. The formation of dark rings has also been observed for gQD/SiO₂ nanostructures. Figures e and f are the original TEM images provided in main text Fig. 1c and d respectively. Both these figures are rotated in the main figure.

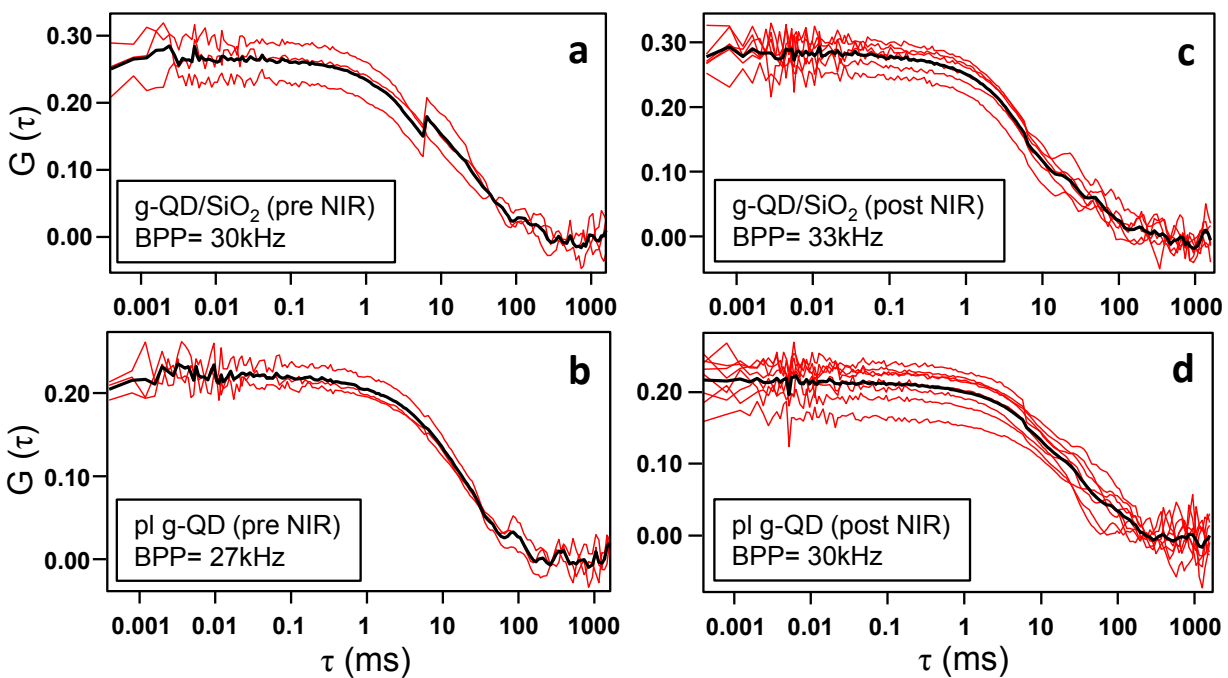


Figure S4. Fluorescence correlation spectroscopy measurements of brightness per particle (BPP) of gQD/SiO₂ and *pl*-gQD (~90% PL retention in Au-coated sample compared to SiO₂-only sample) before and after the near-IR irradiation. No significant change in the BPP was observed after near-IR irradiation.

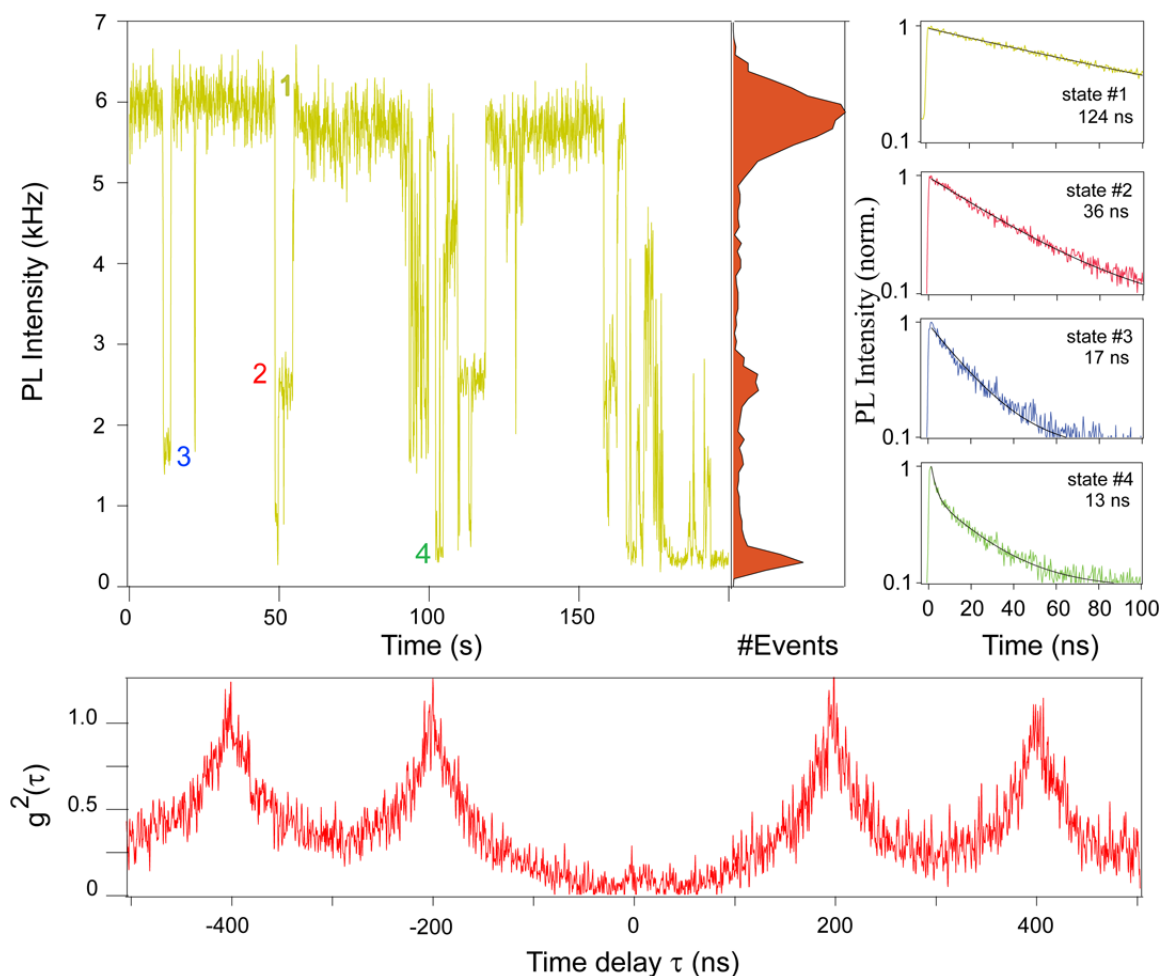


Figure S5. Single-dot blinking trace for a *pl*-gQD comprising a 17 nm SiO₂ spacer layer and a 4-5 nm Au shell. Four distinct emissive states (labeled #1-4) are apparent as indicated by different intensities and PL lifetimes. Bottom: Second-order correlation function $g^2(t) < 0.5$ indicates PL originates from a single nanocrystal, i.e., rather than a cluster. Acquisition conditions: 5 MHz laser excitation pulse rate and average excitation of ~ 0.3 electron-hole pair per dot.

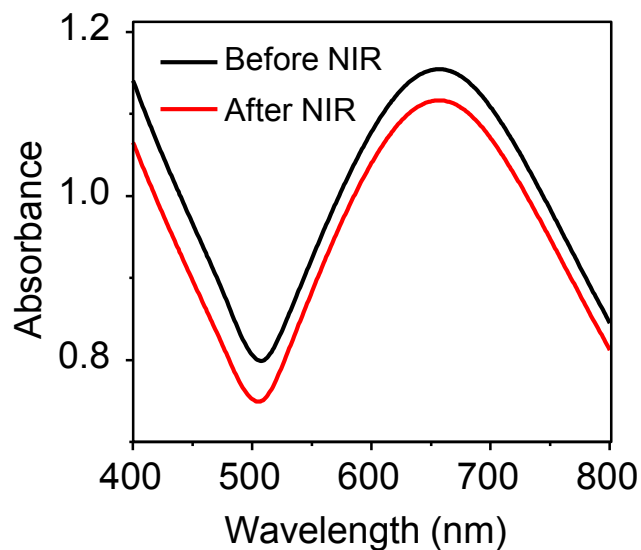


Figure S6. The absorption spectra of the *pl*-gQD before and after the near-IR irradiation. The SPR peak position and peak shape does not change after near-IR exposure.

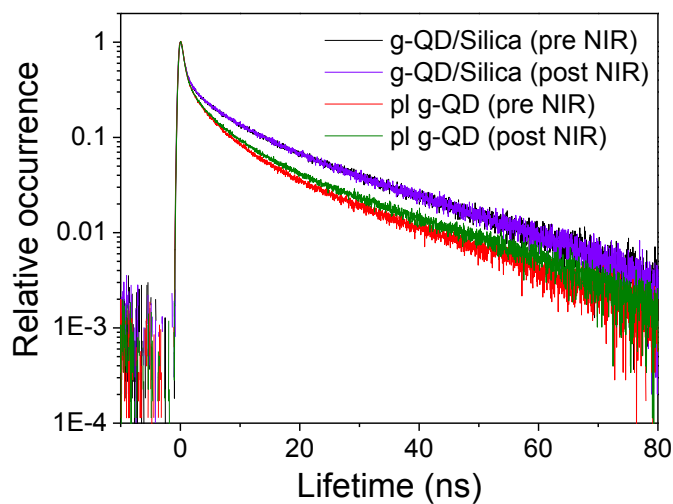


Figure S7. Fluorescence decay lifetime of gQD/SiO₂ and *pl*-gQD before and after near-IR irradiation. Lifetime values do not change significantly following near-IR exposure.

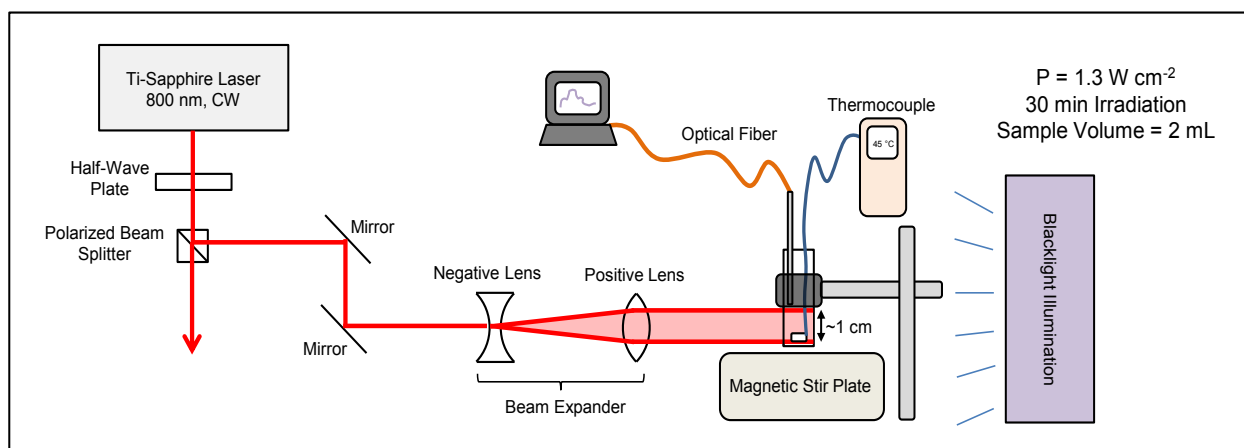


Figure S8. Experimental set up for near-IR induced heating and simultaneous fluorescence measurements of *pl*-gQDs in solution.

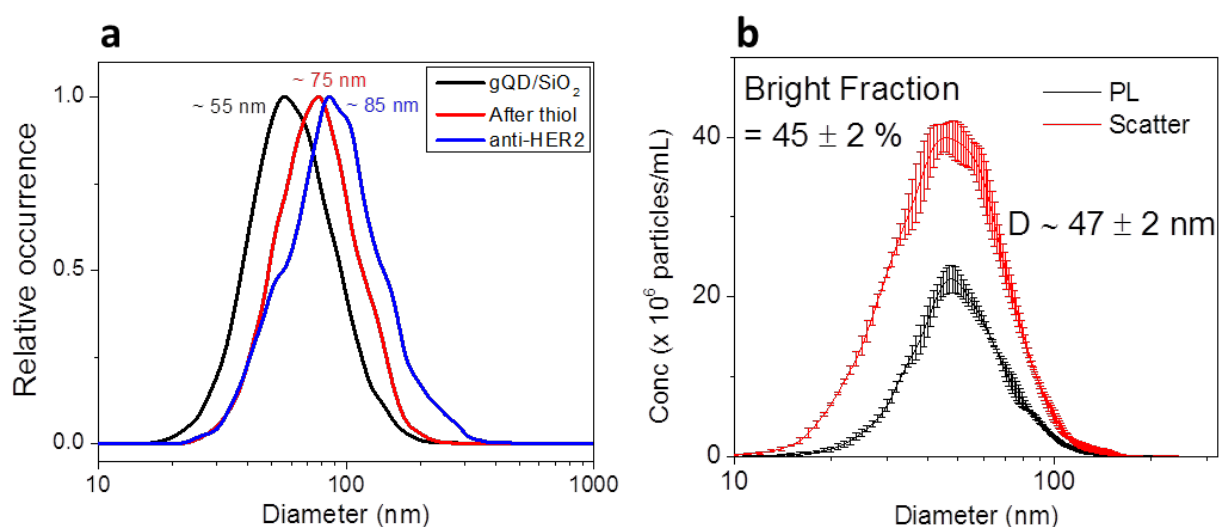


Figure S9. (a) Hydrodynamic diameters (assessed using Nanosight's Nanoparticle Tracking Analysis software) of the gQD/SiO₂ (black curve), *pl*-gQD/PEG₆₀₀₀ (red curve) and anti-HER2-*pl*-gQD/PEG₆₀₀₀ + PEG₆₃₅ (blue curve) products, where the former two samples were suspended in water, while the latter was in cell culture media. In all the cases, hydrodynamic diameter is <100 nm. (b) Bright-dark fraction measurements of water dispersion of gQD/SiO₂ sample done using Nanosight's Nanoparticle Tracking Analysis software.

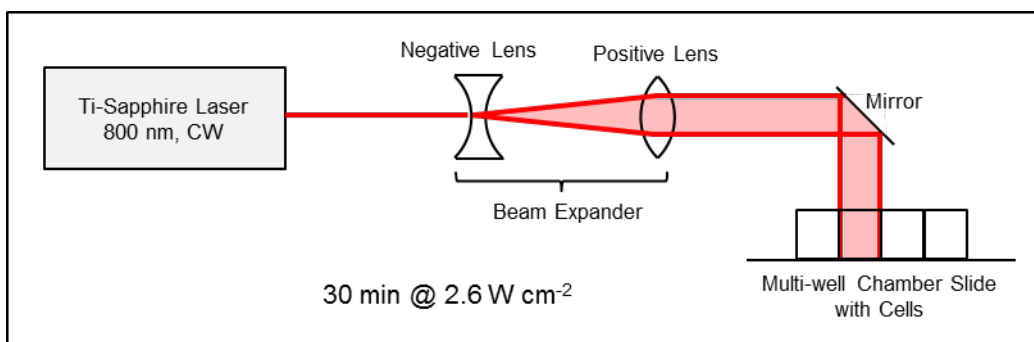


Figure S10. Schematic of experimental setup used for cell heating and thermal ablation experiments.

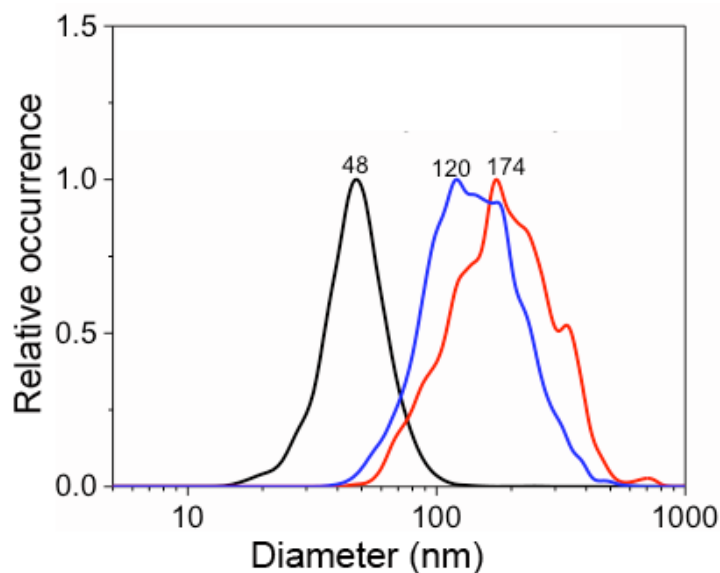


Figure S11. Hydrodynamic diameters (assessed using Nanosight's Nanoparticle Tracking Analysis software) of the gQD/SiO₂ product prior to Au shelling (black trace), as well as after Au shelling in the case of delayed mPEG-thiol addition: ligand addition 1 hr. after Au reduction (blue trace); ligand addition 12 h after Au reduction (red trace).

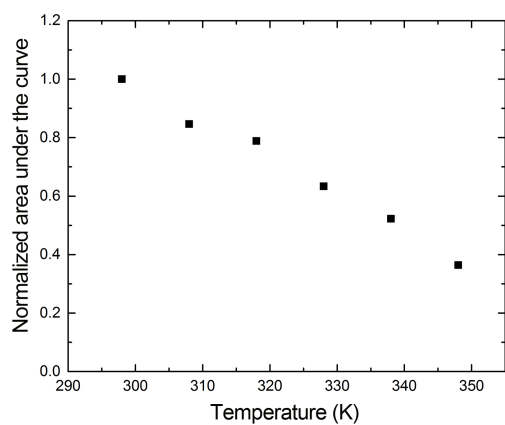


Figure S12. Temperature dependence of *pl*-gQD photoluminescence obtained in pure water to compare to that obtained for gQD/SiO₂ nanoparticles obtained in a water/glycol mixture (main text Figure 4c). Addition of the Au shell does not result in an appreciable difference in thermal quenching behavior.

Supporting References

1. C. K. Chang, Y. J. Chen and C. T. Yeh, *App. Catal. A: General* 1998, **174**, 13-23.
2. J. C. Y. Kah, N. Phonthammachai, R. C. Y. Wan, J. Song, T. White, S. Mhaisalkar, I. Ahmad, C. Sheppard and M. Olivo, *Gold Bull.* 2008, **41**, 23-36.
3. J. D. S. Newman and G. J. Blanchard, *Langmuir* 2006, **22**, 5882-5887.
4. X. Yang, M. Shi, R. Zhou, X. Chen and H. Chen, *Nanoscale* 2011, **3**, 2596-2601.
5. X. Lu, M. S. Yavuz, H.-Y. Tuan, B. A. Korgel and Y. Xia, *J. Am. Chem. Soc.* 2008, **130**, 8900-8901.
6. C.-M. Huang, S.-H. Cheng, U. S. Jeng, C.-S. Yang and L.-W. Lo, *Nano Res.* 2012, **5**, 654-666.
7. Y. Jin and X. Gao, *Nat. Nanotechnol.* 2009, **4**, 571-576.
8. Y. Jin and X. Gao, *J. Am. Chem. Soc.* 2009, **131**, 17774-17776.
9. Y. Jin, C. Jia, S.-W. Huang, M. O'Donnell and X. Gao, *Nat. Commun.* 2010, **1**, 41.